EAA European Acoustics Association

EURONOISE Prague 2012

A simulation-based parameter study of car tyre rolling losses and sound generation

Carsten Hoever, Wolfgang Kropp
Division of Applied Acoustics, Chalmers University of Technology, Gothenburg, Sweden.

Summary
Due to legislative changes within the EU there is an increased demand for improvements in car tyre rolling resistance and noise generation. Apart from measurement data, however, information about the relationship between rolling resistance and rolling noise generation is scarce. It is the goal of this study to investigate the fundamental physical processes connecting both areas. Additionally, it is evaluated whether a simultaneous reduction of both rolling resistance and rolling noise is possible or if this is contradicting requirement. A previously presented model for simulating the structural dynamics and rolling resistance of a rolling car tyre is extended to allow rolling noise calculation. The approach is based on a waveguide finite element model of the tyre. Tyre/road contact forces are obtained using a non-linear 3D contact model. The velocity field on the tyre surface is used to determine the radiated sound pressure based on a boundary element method. In a parameter study it is evaluated how much dissipation and sound radiation are affected by material properties, tyre construction and road surfaces. Due to the characteristics of the modelling approach, detailed information about dissipation and sound generation in different frequency regions, wave orders or parts of the tyre is available. The results show that rolling resistance and radiation are mainly low wave order, low frequency phenomena which are, at least partly, controlled by the same set of modes. This suggests that by modifying specific tyre properties reductions in both sound radiation and rolling resistance can be achieved.

PACS no. 43.20.Mv, 43.20.Rz, 43.40.At, 43.40.Rj, 43.50.Lj

1. Introduction

CO_2 consumption and exterior traffic noise are two major environmental issues associated with the road transportation sector. In 2006 23 % of the CO_2 emissions in the European Union (EU) [1] were due to fuel consumption of road vehicles and it is estimated [2] that about 210 million people are regularly exposed to road traffic noise levels exceeding the WHO guideline value for outdoor sound levels of 55 dB(A) and about 54 million people to road traffic noise levels exceeding 65 dB(A). Approximately 30 % of the fuel consumption is due losses in the tyres and the dominating source mechanism for road traffic noise at the most common driving speeds of 30 km/h to 100 km/h is sound radiation from tyres [3]. Due to this, in November 2012 an EU wide labelling scheme for replacement tyres comes into effect which includes (simplified) information about rolling resistance and sound generation [4]. The goal is to encourage end-users to purchase tyres which are more fuel-efficient and have less external rolling noise.

In spite of the environmental relevance of tyre properties with regard to rolling resistance and sound radiation and the recent effort to put these in a common context, there is astonishingly few detailed information available on the relation between rolling resistance and rolling noise generation of car tyres besides more than a decade old empirical data based on measurements [5, 6].

It is the goal of this study to investigate the fundamental physical processes connecting both areas. Additionally, it is evaluated whether a simultaneous reduction of both rolling resistance and rolling noise is possible or if this is contradicting requirement. For this, a previously presented model for simulating the structural dynamics and rolling resistance of a rolling car tyre [7] is extended to allow rolling noise calculation. The approach is based on a waveguide finite element model (WFEM) of the tyre. Tyre/road contact forces are obtained using a non-linear 3D contact model. The velocity field on the tyre surface is used to determine the radiated sound pressure based on a boundary element method (BEM). In a parameter study it is evaluated how much dissipation and sound

ISSN 2226-5147
ISBN 978-80-01-05013-2

radiation are affected by tyre properties and external parameters such as road surface, speed etc.

Section 2 gives a short overview of the current state of rolling noise and rolling resistance modelling. The simulation framework and the input parameters are shortly described in Section 3. Sections 4 to 6 contain results for the standard tyre/road configuration and the findings of the parameter study. Finally, the results are summarised and concluding remarks are given in Section 7.

2. On rolling resistance and sound radiation

Rolling resistance is defined as the mechanical energy converted into heat for a unit distance travelled in J/m [8]. This allows the use of the term *rolling loss* as an equivalent expression for *rolling resistance*.

The greatest part of rolling losses can be attributed to hysteresis. During rolling, the tyre material is periodically deformed. Due to the viscoelastic properties of the rubber compound, not all of the stored elastic energy can be regained in each cycle, instead a part of it is dissipated. The main cause of deformation for a rolling tyre is the flattening of the contact patch, causing bending of the crown, the sidewalls and the bead area, compression of the tread and shearing of the tread and the sidewall [9]. This leads to a propagation of disturbances inside the tyre structure as waves in a variety of different mode shapes and orders, ultimately resulting in dissipation and sound radiation.

While the relationship between rolling resistance and typical tyre parameters (such as pressure, load, speed, etc.) has been well documented [10, 11], and several examples of rolling noise calculations can be found [12, 13, 14], information on the relation between rolling resistance and rolling noise generation is scarce. Extensive experimental data obtained by several authors (cf. [5, 6]) suggests that there is no incompatibility between simultaneous noise and rolling resistance improvements. However, due to the empirical nature of the results, not much insight into the physical processes has yet been obtained.

Though numerous examples for calculations of rolling resistance are available in the literature, the models used are often over-simplified (e.g. [15, 16]) and/or based on modelling approaches which do not readily allow identification of connections to the structural dynamics (and hence the rolling noise) of the tyre [17, 18, 19].

Bschorr and Wolf [20] seem to be the first to have used a model of the tyre's structural dynamics to draw conclusions about the rolling resistance. However, their rolling resistance estimation was not very detailed as it was merely a by-product of their study on tyre vibrations. Kim and Savkoor [21] used a model of an elastic ring supported by a viscoelastic foundation to calculate the rolling resistance for a free-rolling tyre. While the same model could be used to draw simplified conclusions about the rolling noise as well, this was not done. More recently, Boere *et al.* [22] investigated the influence of different road textures on rolling noise and rolling resistance. However, with the main focus being on the impact of the tyre/road interaction, there was no examination of the physical processes in the tyre.

A substantial contribution was made by Fraggstedt [24] when he developed a waveguide finite element model of a car tyre for calculating the vibrations and rolling losses of a rolling tyre. Due to the nature of the WFEM approach, the results are detailed and physically easy to interpret. On the downside, rolling resistance and tyre vibrations were not analysed in a common context, but independently from each other for different cases. As radiation was not included in the model, rolling noise could not be calculated.

Rolling noise simulations have so far been basically restricted to evaluations of road texture influence [12], the horn-effect [13] or the identification of dominating radiation processes [14].

To establish a common context for the evaluation of rolling resistance and rolling noise, available simulation procedures for the calculation of rolling losses [7] and sound radiation [14] are combined, facilitating the identification of similarities and differences in the underlying dynamical mechanisms leading to both phenomena.

3. Modelling procedure

The simulation framework is in huge parts identical to the one previously described in [7]. Starting point is a 205/55R16 slick tyre which is modelled using a waveguide finite element approach which combines FE modelling of the cross-section with a wave ansatz for the circumference, resulting in a unique eigenvalue problem for each of the circumferential wave orders. Tyre/road interaction is modelled using a non-linear 3D approach which accounts for the alternating relation between contact forces and tyre vibrations and is based on 3D scans of road surfaces and real tyre geometries. Contrary to the previously presented approach, the contact problem formulation has been changed to

$$\mathbf{u}(t) = \mathbf{C} \cdot \mathbf{F}(t) + \tilde{\mathbf{u}}(t) \tag{1a}$$

$$F_i(t) = k \cdot d_i(t) \cdot \mathcal{H}\{d_i(t)\} \tag{1b}$$

$$\mathbf{d}(t) = \mathbf{z}_R(t) - \mathbf{z}_T(t) - \mathbf{u}(t)\,. \tag{1c}$$

Herein, $\mathbf{u}$ denotes the normal tyre displacements, $\mathbf{C}$ is an influence matrix obtained from the first value of the tyre's Green's function, $\mathbf{F}(t)$ denotes the normal contact forces for all contact points and $\tilde{\mathbf{u}}$ the displacement given by the contribution of the whole contact time history. k is a penalty spring stiffness,

$\mathcal{H}$ is the Heaviside function, $\mathbf{z}_R$ and $\mathbf{z}_T$ are the road surface and tyre profile height above a reference level and $\mathbf{d}(t) \geq 0$ is the distance between a tyre surface and road. By obtaining the influence matrixes directly from the tyre's Green's function the viscoelastic properties of the tread are better represented than with the previously used elastic half-space formulation. Another change is the use of penalty springs which account for contact stiffness changes due to differences between apparent and real area of contact. Further information about the contact model can be found in [23].

Due to energy conservation, rolling losses can be calculated as input power for steady-state rolling conditions. As shown in [24] the time averaged input power for a WFE tyre model is

$$P_{in} = 2\pi \sum_{n=-N}^{N} \sum_{m=0}^{M} j\omega_m [\hat{\mathbf{F}}_{-n}^{H}(\omega_m) \cdot \hat{\mathbf{v}}_{-n}(\omega_m) - \hat{\mathbf{F}}_{n}^{T}(\omega_m) \cdot \hat{\mathbf{v}}_{n}^{*}(\omega_m)] \,. \quad (2)$$

$\hat{\mathbf{F}}$ and $\hat{\mathbf{v}}$ are the nodal forces and displacements, $j = \sqrt{-1}$ and the summation is done over wave orders $\pm n$ in positive and negative circumferential direction and the frequencies ω_m. $(\bullet)^*$ denotes the complex conjugate, $(\bullet)^T$ matrix transpose and $(\bullet)^H = (\bullet)^{T*}$. Equation (2) conveniently allows the identification of the contribution of individual wave orders or frequencies to the rolling losses. If ones uses $\hat{\mathbf{F}}_n(\omega_m) = \mathbf{D}_n(\omega_m)\hat{\mathbf{v}}_n(\omega_m)$ in (2), where $\mathbf{D}_n(\omega_m)$ consists of the stiffness and mass matrices, dissipation can be calculated element-wise. This allows to identify the spatial dissipation distribution over the tyre cross section.

Radiation calculations are based on a half-space BEM approach which models the reflection on the road surface using specially derived Green's functions [25]. To include the influence of the horn effect, the BEM mesh includes the tyre deformation due to static loading in the contact region. The radiation is evaluated as mean sound pressure at 321 points on a half-sphere of radius 1 m around the contact point between tyre and road. A total A-rated sound pressure level is calculated for the third-octave bands from 200 Hz to 2000 Hz.

The tyre mesh consists of 20 solid elements for the tread and 46 shell elements for the sidewalls and belt, see Figure 1. The resolution around the tyre circumference is 512 steps. The rim and the air cavity are not explicitly modelled, but their effect is included by blocking the tyre motion at the bead and including the pre-tension due to inflation. Damping is implemented using complex values for different stiffness and pretension components, with loss factors of 0.01 to 0.1 for the shell stiffnesses, 0.01 to 0.05 for shell pretension and 0.25 for the solids in the highly damped tread. Details about the other material parameters can be found in [23].

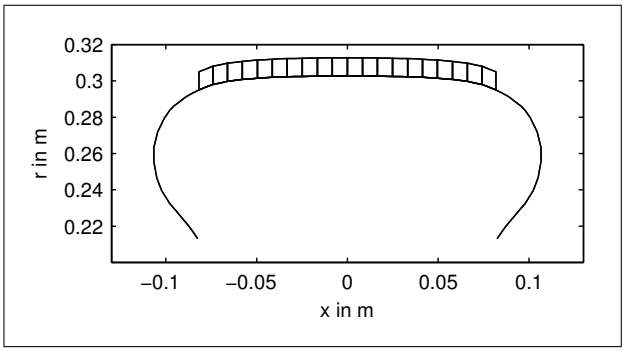

Figure 1. WFEM mesh of the tyre cross section.

Table I. Overview of variation of tyre independent parameters in study A. Standard configuration marked bold.

Parameter	Values
speed	**50 km/h**, 80 km/h, 110 km/h
static load	2500 N, 3000 N, **3415 N**, 4000 N, 4500 N
road surface	**ISO 10844**, rough
temperature	**20 °C**, 55 °C

For the basic configuration a driving speed of 50 km/h and a static load of 3415 N are used. The road roughness profile is based on a 3D scan of 15 lateral tracks of a drum-mounted ISO 10844 road surface. Rolling is calculated for six full tyre revolutions of which the last two are evaluated, resulting in a frequency resolution of 3.5 Hz for the 50 km/h case. The described modelling procedure has been validated in [23].

The parameter study is divided into two parts: study A, in which tyre independent parameters such as speed, static load, road surface etc. are varied and study B, which investigates changes to tyre construction and material properties. For a detailed overview see Tables I and II. Regarding the variations of mass (distribution) it has to be added that these are obtained by density changes which leave the rest of the tyre construction, including the geometry, unchanged. In total, rolling losses are calculated for 51 configurations and additionally for 32 of these the rolling noise is calculated as well.

4. Results basic configuration

The basic configuration leads to rolling losses of 317 W. Figure 2 shows the distribution of losses over frequency and wave order, revealing that most dissipation occurs for low frequencies and wave orders. The colour plot reveals that the dissipation exclusively occurs for frequency and wave order combinations which form a straight line, i.e. each wave order can be unambiguously related to a specific frequency. As shown

Table II. Overview of variation of tyre dependent parameters in study B. Listing of original configuration (i.e. 100 %) omitted for all cases.

Parameter	Variation
stiffness sidewall	50 %, 75 %, 150 %, 200 %
stiffness belt	50 %, 75 %, 150 %, 200 %
shell stiffness	50 %, 75 %, 150 %, 200 %
Young's mod. tread	50 %, 75 %, 150 %, 200 %
pretension	50 %, 75 %, 150 %, 200 %
mass	75 %, 87.5 %, 112.5 %, 125 %
mass distribution	towards sidewalls, towards tread, equal
loss factor	50 %, 75 %, 150 %, 200 %
geometry	rounder, flatter, thicker tread

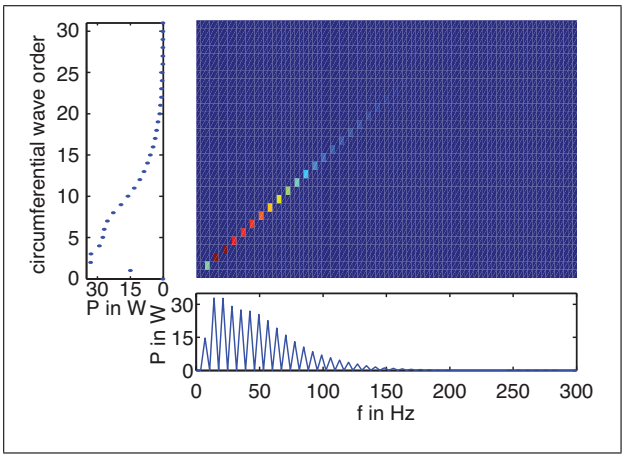

Figure 2. Dissipated power for the original configuration as a function of frequency (bottom) and circumferential wave order (left) and as combined colour plot. Colour is re. maximum of plot.

in [7] this frequency is given by the forced excitation of the tyre. This also means that free wave propagation does not contribute significantly to the dissipation.

Figure 8 shows the radiated sound pressure level for the basic configuration. It reveals the typical peak for third-octave bands from 1 kHz to 1.6 kHz. A detailed analysis and comparison with measurement results can be found in [14], where it is also shown that rolling noise strongly depends on lower order waves. As a similar lower order dependancy of rolling losses is shown in Figure 2, a possible link between the physical processes behind rolling losses and sound radiation is found.

5. Results parameter study

In this section the preliminary results of the parameter studies A and B are presented. Figures 3 und 4

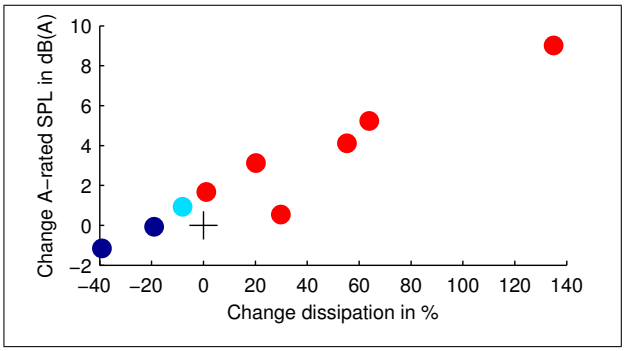

Figure 3. Results parameter study for tyre independent parameters. + original configuration. Colours identify different combinations of increase/decrease of rolling noise/rolling resistance.

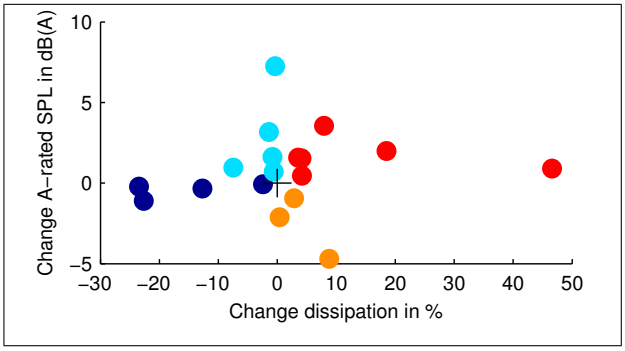

Figure 4. Results parameter study for tyre parameters. + original configuration. Colours identify different combinations of increase/decrease of rolling noise/rolling resistance.

show the total changes of rolling loss and rolling noise in comparison to the original configuration. For the variation of tyre independent parameters in study A, Figure 3 shows a correlation of rolling noise reduction (increase) with rolling loss reduction (increase) for all but one case. This is in line with the experimental results obtained in [5, 6].

For changes of tyre parameters in study B, results are more inhomogeneous, see Figure 4. In the obtained "crosswise" distribution of results the horizontal axis with strong changes of rolling resistance and only slight changes of radiation is based exclusively on changes of tyre belt and sidewall stiffness and the pretension. The vertical axis with strong rolling noise changes but marginal rolling loss changes only contains configurations in which the mass respectively the mass distribution of the tyre are changed.

6. Detailed analysis

Within the scope of this article a detailed analysis of all configurations is not possible, instead the three configurations shown in Table III are exemplarily chosen and analysed in detail in the following. The configurations for changed pretension and shell stiffness are

Table III. Results for the three example configurations. Negative values denote reduction.

Configuration	ΔP_{diss}	ΔSPL
pretension +50 %	-22.7 %	-1.1 dB(A)
shell stiffness +100 %	-12.6 %	-0.4 dB(A)
mass +25 %	+0.3 %	-2.1 dB(A)

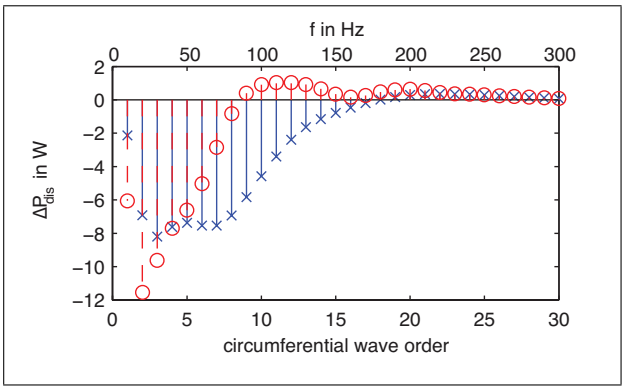

Figure 5. Change in dissipated power over circumferential wave order/frequency compared to original configuration for (—×) pretension +50 %, (– –○) shell stiffness +100 %. Negative values denote reduction. Note: Double x-axis due to fixed relation between wave order and frequency for forced excitation.

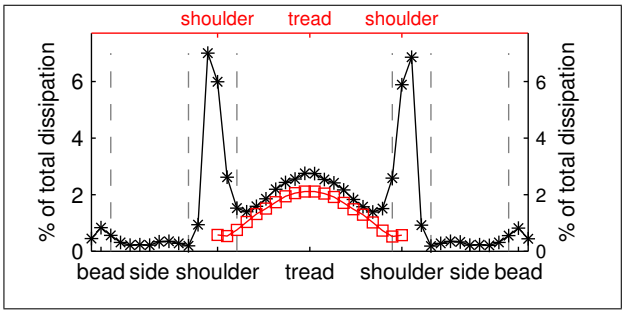

Figure 6. Distribution of dissipation over tyre cross section for pretension +50 %. Shell elements in black, solid elements in red. (– –) marks different tyre regions.

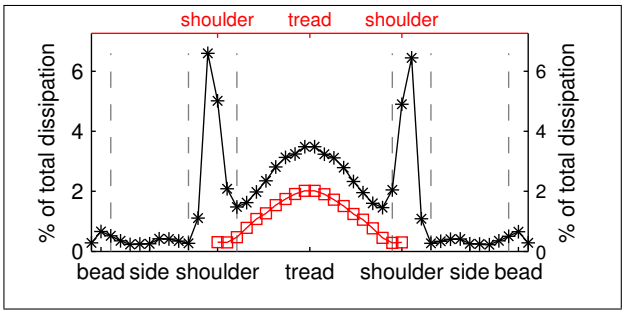

Figure 7. Distribution of dissipation over tyre cross section for shell stiffness +100 %. Shell elements in black, solid elements in red. (– –) marks different tyre regions.

examples for cases which mainly effect rolling losses. Yet, as will be shown, there are differences in detailed results. The mass reduction is an example for a configuration mainly affecting rolling noise.

Figure 5 shows that though the changes in pretension and shell stiffness both lead to overall reduction of rolling losses (albeit to a different extent), to which degree individual frequencies and wave orders are affected differs considerably. For increased pretension the reduction seems to be proportional to the original distributions as shown in Figure 2. The effect of the change in stiffness in contrast, is most prominent for frequencies 14 Hz and 21 Hz, and wave orders 2 and 3, while for frequencies above 60 Hz and wave orders higher than 8 rolling losses are actually higher than for the original configuration. Differences are also visible in the cross-section distribution of rolling losses shown in Figures 6 and 7, especially in the contribution of the shell elements in the tread region.

In Figure 8 the radiated sound pressure of the configurations with higher mass and higher pretension are compared with the original configuration. For the increased mass, the reduction is mainly limited to the dominating region at and above 1 kHz. For lower frequencies the curve is nearly identical to the original case with the exception of 800 Hz, where it is higher. For higher pretension, the radiated sound pressure level is equal to or even higher than in the original configuration for all third-octave bands but those with centre frequencies 800 Hz, 1 kHz and 1.6 kHz. Still, the overall A-rated SPL is 1.1 dB lower than in the basic configuration.

A possible explanation for the differences might be that in the mass case the tyre excitation is not affected (as indicated by the nearly unchanged rolling resistance), whereas the propagation of the structural waves on the tyre which cause radiation is affected. In case of the pretension change, excitation of low order waves might be influenced. This not only considerably affects rolling losses as shown in Section 4, but according to the results in [14] also the rolling noise in the dominating region from 1 kHz to 2 kHz. Hence, a noticeable reduction is achieved for both criteria for the case of increased pretension. The increased shell stiffness seems to have a more localised effect in terms of affected frequencies and wave orders which needs further investigations before conclusions can be drawn.

7. Conclusions

The results show that there is no general contradiction between concurrent reductions of rolling resistance and exterior rolling noise. In fact for many cases there is a correlation between both quantities. The parameter study indicates that by modification of certain tyre parameters a simultaneous decrease of rolling losses and sound radiation can be achieved. In this regard, low wave orders, which are fundamental to rolling re-

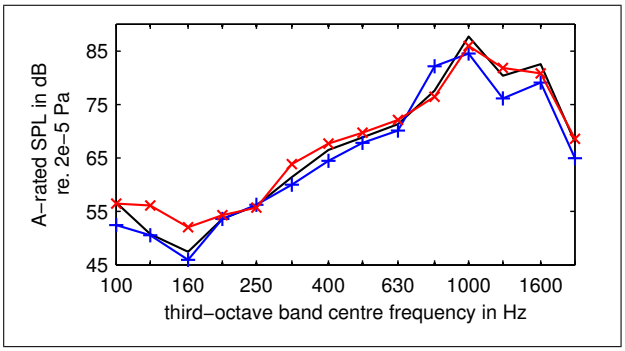

Figure 8. Rolling noise in third-octave bands for (—) original configuration, (-+-) mass +25 %, (− × −) pretension +50 %.

sistance and sound radiation in the dominant region above 1 kHz, are particularly important. The analysis has been limited to a selective modification of individual tyre properties. Whether the more common case of changing several tyre properties at a time leads to different relations between rolling resistance and radiation has to been shown in further investigations.

The study also shows that despite substantial changes in tyre design are made, changes in radiated sound pressure levels are rather limited; typically in the range of 1 dB to 2 dB. Combining changes of multiple material properties together with geometrical modifications might be needed to achieve higher reduction. This potential has to be explored further.

References

[1] Annual EC greenhouse gas inventory 1990–2006 and inventory report 2008. Report No 6/2008, EC, EPA, 2008.

[2] L. den Boer, A. Schroten: Traffic noise reduction in Europe. CE Delft, 2007.

[3] W. van Keulen, M. Duškov: Inventory study of basic knowledge on tyre/road noise. Report DWW-2005-022, IPG, 2005.

[4] Regulation (EC) No 1222/2009. EC Official Journal L **342** (2009), 46–58.

[5] U. Sandberg, J.A. Ejsmont: Noise emission, friction and rolling resistance of car tires - Summary of an experimental study. Proc. NOISE-CON 2000.

[6] R. Stenschke, P. Vietzke: Noise and use characteristics of modern car tyres (State of the art). Proc. 7th ICSV 2000, 2781–2788.

[7] C. Hoever, P. Sabiniarz, W. Kropp: Waveguide-finite-element based parameter study of car tyre rolling losses. Proc. 6th Forum Acusticum 2011, 789–794.

[8] ISO 18164:2005 Passenger car, truck, bus and motorcycle tyres — Methods of measuring rolling resistance.

[9] The pneumatic tire. U.S. Department of Transportation, 2006.

[10] S. Bandyopadhyay, A. Chandra, R. Mukhopadhyay: An overview of tyre rolling loss. Progress in rubber and plastics technology **10** (1994) 20–53.

[11] Tires and passenger vehicle fuel economy. Report 286, Transportation Research Board, 2006.

[12] M. Brinkmeier, U. Nackenhorst, S. Petersen, O. von Estorff: A finite element approach for the simulation of tire rolling noise. Journal of Sound and Vibration **309** (2008) 20–39.

[13] W. Kropp, F.-X. Becot, S. Barrelet: On the sound radiation from tyres. Acta Acustica united with Acustica **86** (2000) 769–779.

[14] W. Kropp, P. Sabiniarz, H. Brick, T. Beckenbauer: On the sound radiation of a rolling tyre. Journal of Sound and Vibration **331** (2012) 1789–1805.

[15] D. Stutts, W. Soedel: A simplified dynamic model of the effect of internal damping on the rolling resistance in pneumatic tires. Journal of Sound and Vibration **155** (1992) 153–164.

[16] R. Brancati, S. Strano, F. Timpone: An analytical model of dissipated viscous and hysteretic energy due to interaction forces in a pneumatic tire: Theory and experiments. Mechanical Systems and Signal Processing **25** (2011) 2785–2795.

[17] Y. Lin, S. Hwang: Temperature prediction of rolling tires by computer simulation. Mathematics and Computers in Simulation **67** (2004) 235-249.

[18] H. Park, S.-K. Youn, T. Song, N.-J. Kim: Analysis of temperature distribution in a rolling tire due to strain energy dissipation. Tire Science and Technology **25** (1997) 214–228.

[19] L.H. Yam, J. Shang, D.H. Guan, A.Q. Zhang: Study on tyre rolling resistance using experimental modal analysis. International Journal of Vehicle Design **30** (2002) 251-262.

[20] O. Bschorr, A. Wolf: Reifenschwingungen als Ursache von Lärm und Rollwiderstand. Automobil-Industrie **27** (1982) 451–458.

[21] S. Kim, A. Savkoor: The contact problem of in-plane rolling of tires on a flat road. Vehicle System Dynamics **27** (1997) 189–206.

[22] S. Boere, I. Lopez, A. Kuijpers, H. Nijmeijer: Prediction of road texture influence on rolling resistance and tyre/road noise. Proc. Euronoise 2009.

[23] P. Sabiniarz: Modelling the vibrations on a rolling tyre and their relation to exterior and interior noise. PhD thesis, Chalmers Univ. of Techn., Gothenburg, 2011.

[24] M. Fraggstedt: Vibrations, damping and power dissipation in car tyres. PhD thesis, Royal Inst. of Sciences, Stockholm, 2008.

[25] H. Brick: Application of the Boundary Element Method to combustion noise and half-space problems. PhD thesis, Chalmers Univ. of Techn., 2009.